References and Notes

1. D. S. Saunders, *Insect Clocks* (Pergamon, Oxford, 1976).
2. H. P. Leinaas, *Z. Zool. Syst. Evolutionsforsch.* **19**, 278 (1981).
3. J. Mertens and R. Bourgoignie, *Behav. Ecol. Sociobiol.* **2**, 41 (1977).
4. H. P. Leinaas, in preparation.
5. E. O. Wilson, *The Insect Societies* (Harvard Univ. Press, Cambridge, Mass., 1971).
6. M. J. Richards and M. A. Mangoury, *Nature (London)* **219**, 865 (1968); M. S. Blum, in *Pheromones*, M. C. Birch, Ed. (North-Holland, Amsterdam, 1974), pp. 190–199.
7. G. Rakowski and B. Cymborowski, *Int. J. Invertebr. Reprod.* **4**, 249 (1982). They also report that the pheromone from adults maintains synchronized moulting in a group of larvae already synchronized. A similar group of larvae not exposed to adult pheromone became less synchronized over succeeding moults. Because exposure of unsynchronized larvae (and different instars) to the pheromone was not tested, it is not clear whether the synchronization is a secondary effect of moult inhibition or an adaptive trait of the pheromone system.
8. C. Van der Kraan, *Rev. Ecol. Biol. Sol* **8**, 99 (1971); W. H. Lyford, *Am. Midl. Nat.* **94**, 205 (1975); H. R. Simon, *Entomol. Z.* **85**, 89 (1975).
9. A. Semb-Johansson, *Norsk Entomol. Tidsskr.* **7**, 145 (1951).

10. I thank K. B. Døving, A. Løvlie, J. G. Ormerod, L. Sømme, K. E. Zachariassen, and A. Semb-Johansson for commenting on the manuscript, E. Bleken for inspecting the cultures at times when I was away, and L. Fusdahl for typing the manuscript.

30 June 1982

Myasthenic Globulin Enhances the Loss of Acetylcholine Receptor Clusters

Abstract. *Acetylcholine receptors are present in the sarcolemma of cultured skeletal muscle myotubes either as large clusters or in a diffuse distribution. Both the clustered and diffuse acetylcholine receptors are potentially removable from the membrane. Treatment of myotubes with globulin from patients with myasthenia gravis causes the loss of acetylcholine receptor clusters and the concomitant appearance of acetylcholine receptor microaggregates. The rate of acetylcholine receptor cluster loss is greater than the rate of acetylcholine receptor degradation, indicating that acetylcholine receptors are disrupted from clusters to form microaggregates before being removed from the plasma membrane.*

The distribution of acetylcholine receptors (AChR's) in cultured myotubes is not uniform. Areas of sarcolemma containing clusters of AChR's ("hot spots") and high sensitivity to iontophoretically applied acetylcholine (ACh) have been found both in vitro and in vivo (*1*). Studies of AChR turnover rate monitored with ^{125}I-labeled α-bungarotoxin (α-BTX), a neurotoxin that binds to the AChR essentially irreversibly, have demonstrated that the half-life of AChR's in myotube cultures is 18 to 24 hours (*2*).

To gain a better understanding of the process by which AChR's are removed, we have investigated AChR cluster morphology under conditions of enhanced AChR turnover. Antibodies to AChR from patients with myasthenia gravis (MG) were used to accelerate AChR degradation (*3*). We used a fluorescent conjugate of α-BTX to locate AChR clusters (*4*) in cultures of rat myotubes after incubating the cultures with antibodies from MG patients. Our studies demonstrate that the number of AChR clusters is greatly reduced in cultures incubated with immunoglobulin from MG patients (MG globulin). At the same time microaggregates (*4*) of AChR appear over a wide area of the sarcolemma. Both of these events occur faster than AChR degradation.

Experiments were carried out on cultured rat myotubes (*5*). Cells were plated in Falcon tissue culture dishes containing glass cover slips. Cultures were grown at 37°C under an atmosphere of 5 percent CO_2 and 95 percent air. The receptor distribution was examined by staining the cultures with a tetramethylrhodamine conjugate of α-BTX (α-BTX-TMR) (*6*). This technique is specific for detection of AChR's, allowing us to visualize AChR clusters. Cells first incubated with unlabeled α-BTX and then with α-BTX conjugate show a complete absence of label.

Cells were incubated for 1 hour at 37°C with $5 \times 10^{-8} M$ α-BTX-TMR, rinsed, and incubated with MG globulin or normal globulin for 0 to 6 hours. Other cultures were stained after the addition of MG globulin or normal globulin at 37° or at 4°C to determine (i) whether the distribution of microaggregates is similar to that seen when cells are stained before the addition of immunoglobulin and (ii) whether the redistribution of microaggregates can be seen when cells are stained at 4°C.

Cells were fixed in 2 percent buffered formaldehyde and examined in a Zeiss microscope equipped with incident-light fluorescence optics and with phase-contrast optics. Purified globulin from patients with MG that had high titers for antibody to AChR (demonstrated with radioimmunoassay) was used in all experiments (*7*). The number of myotubes containing intact AChR clusters (*4*) and the number of myotubes containing microaggregates (*4*) were counted in random microscopic fields. The number of intact clusters was defined as the ratio of the number of myotube segments containing intact clusters to the number of

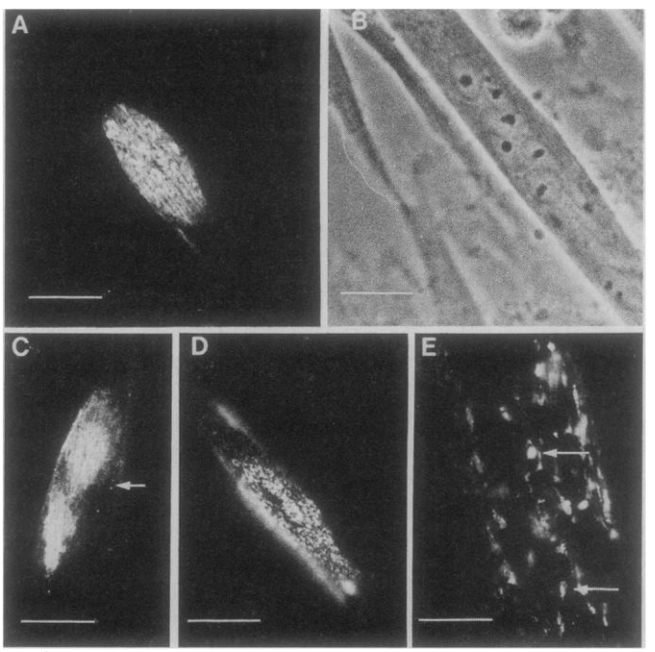

Fig. 1. Rat myotubes were grown on collagen-coated glass cover slips, washed, and stained with fluorescent α-BTX ($5 \times 10^{-8} M$) for 1 hour at 37°C. Cultures were incubated in normal globulin or MG globulin, fixed in 2 percent phosphate-buffered formaldehyde, and observed and photographed with a Zeiss fluorescent microscope. All micrographs were exposed, developed, and enlarged identically (×400). (A) Myotube incubated with normal globulin for 6 hours. An intensely fluorescent intact cluster is present. (B) Phase-contrast image of the myotube in (A). The fluorescent cluster seems to be localized over nuclei. (C) Myotube incubated with MG globulin for 5 minutes and fixed in formaldehyde. A few speckles (arrows) are close to the intact fluorescent cluster. (D) Myotubes exposed to MG globulin for 3 hours show an AChR cluster that is no longer densely packed. (E) Myotube incubated with MG globulin for 6 hours shows complete dissolution of the AChR cluster. Microaggregates 2 to 6 μm in diameter (arrows) are present. Scale bar, 20 μm.

myotubes containing either intact clusters or microaggregates, or both. Myotubes containing both intact clusters and microaggregates were scored separately for each parameter. The AChR cluster loss was determined from the decrease in the number of intact clusters with time. The degradation rate of AChR in cell culture in the presence and absence of MG globulin was determined with ^{125}I-labeled α-BTX ($2 \times 10^{-8} M$) and assayed as described (*2, 3*).

Control myotubes incubated with α-BTX-TMR at 37°C for 1 hour displayed intensely fluorescent clusters, usually 20 to 60 μm in length. Cultures treated with normal human globulin for 5 minutes to 6 hours show similar intact fluorescent clusters (Fig. 1A). The clusters do not present a smooth appearance, but rather exhibit a series of strands (Fig. 1A), as also reported by others (*8*). Fluorescent images of AChR clusters are frequently seen in close approximation to nuclei viewed with phase-contrast optics (*9*) (Fig. 1B). Myotubes incubated with MG globulin show a time-dependent loss of AChR clusters. Five minutes after exposure to MG globulin, evidence for cluster disruption is seen (Fig. 1C); after incubation with MG globulin for 3 hours, myotubes show a granular, grapelike appearance (Fig. 1D); and after incubation for 6 hours, myotubes show loss of AChR clusters, and the linear organization of AChR clusters is no longer observed. These cells have small (2 to 6 μm^2) microaggregates (*4*) that are distributed throughout the myotube (Fig. 1E). A similar distribution of microaggregates was observed when cultures were stained with α-BTX-TMR at 4°C after exposure to MG globulin, suggesting that the microaggregates are located on the cell surface. The decrease in the number of AChR clusters coincides with the increase in the appearance of microaggregates (Fig. 2).

The decrease in the percentage of clusters was compared with the loss of ^{125}I-α-BTX binding sites (*2*). After the myotubes were incubated with MG globulin for 6 hours, 50 ± 2 percent of the initial ^{125}I-α-BTX binding sites remained intact, whereas only 25 ± 9 percent of the AChR clusters remained intact ($P < .001$ by modified *t*-test) (*10*). Thus, in the presence of MG globulin the loss of AChR clusters is about 1.5 times the rate of AChR degradation. This effect is not the result of a complement-related process, because we used purified globulin. A loss of AChR clusters was also observed in untreated cultures and cultures treated with normal globulin but at a much slower rate (Fig. 2). This redistribution is not caused by α-BTX (*1*), or the dissociation of the chromophore from the toxin-AChR complex. Cultures fixed before or after exposure to α-BTX-TMR and left at 37°C for up to 24 hours show intact intensely fluorescent clusters. After fixation, loss of clusters was not observed.

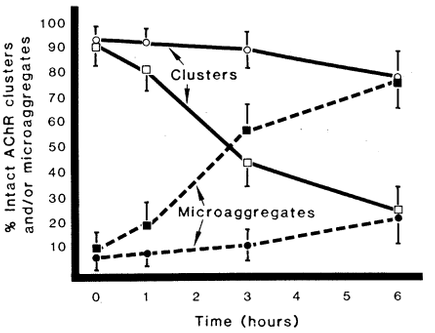

Fig. 2. The percentage of AChR clusters remaining after treatment with normal globulin (open circles) and MG globulin (open squares) at indicated times. Under normal culture conditions, about half of the myotubes contained AChR clusters. The decrease in the percentage of myotubes containing intact AChR clusters after treatment with MG globulin is accompanied by an increase in the percentage of myotubes containing microaggregates (closed squares). Closed circles denote the percentage of myotubes containing microaggregates after treatment with normal globulin. Each point indicates the mean ± standard deviation (bars) determined from 20 microscopic fields in each of three cultures. For each point, 30 to 40 myotubes containing AChR clusters or AChR microaggregates, or both (*4*), were counted. The average value for the percentage of intact clusters remaining is significantly different ($P < .001$) 1, 3, and 6 hours after MG globulin treatment.

We have found that MG globulin not only increases the turnover rate of AChR's, but also increases the rate of AChR cluster loss. In cultures treated with MG globulin, the calculated rate of AChR cluster loss is greater than the rate of total AChR degradation, whereas in cultures treated with normal globulin, the rate of AChR cluster loss is less than the rate of AChR degradation. One possible explanation is that MG antibody disrupts the AChR clusters, thereby leading to the appearance of microaggregates (Fig. 1E). These microaggregates may be the specialized domains of plasma membrane at which internalization of AChR rapidly occurs, perhaps via the coated pit mechanism (*11*). Another possible explanation is that the microaggregates are the result of cross-linking of diffuse AChR molecules that can migrate in the plane of membrane (*12*).

Evidence for the first possibility includes the following. (i) Under normal culture conditions, 92 percent of AChR clusters are intact rather than dispersed. (ii) The disappearance of AChR clusters coincides with the appearance of microaggregates and with the increased degradation rate of AChR. (iii) The disappearance of AChR clusters after MG globulin treatment occurs faster than the removal of total surface AChR as measured by ^{125}I-α-BTX. Although we have not followed individual clusters through stages of cluster loss, our observations indicate that cluster loss is a gradual process. If the rate of AChR cluster loss is sufficiently slow, AChR internalization may occur at intact clusters, thus explaining the observation that degradation occurs faster than cluster loss in control cultures. Whether internalization of the AChR-α-BTX complex takes place at AChR clusters, or whether AChR's are internalized randomly throughout the sarcolemma remains to be determined. Our study indicates that AChR's are not structurally fixed in clusters and that cluster disruption may precede AChR internalization when AChR turnover is enhanced by MG antibody.

SHERRY BURSZTAJN*
JAMES L. MCMANAMAN
STANTON B. ELIAS
STANLEY H. APPEL

Department of Neurology and Program in Neuroscience, Jerry Lewis Neuromuscular Disease Research Center, Baylor College of Medicine, Houston, Texas 77030

References and Notes

1. M. J. Anderson and M. W. Cohen, *J. Physiol. (London)* **268**, 757 (1977); _____, E. Zorychta, *ibid.*, p. 731; D. Axelrod, P. Ravdin, D. E. Koppel, J. Schlessinger, W. W. Webb, E. L. Elson, T. R. Poleski, *Proc. Natl. Acad. Sci. U.S.A.* **73**, 4594 (1976); G. D. Fischbach and S. A. Cohen, *Dev. Biol.* **31**, 147 (1973); A. J. Sytkowski, Z. Vogel, M. W. Nirenberg, *Proc. Natl. Acad. Sci. U.S.A.* **69**, 3180 (1972); P. K. Ko, M. J. Anderson, M. W. Cohen, *Science* **196**, 540 (1977).
2. P. N. Devrotes and D. M. Fambrough, *J. Cell Biol.* **65**, 335 (1975); P. N. Devrotes, J. M. Gardner, D. M. Fambrough, *Cell* **10**, 365 (1977).
3. S. H. Appel, R. Amwyl, M. W. McAdams, S. Elias, *Proc. Natl. Acad. Sci. U.S.A.* **74**, 2130 (1977); I. Kao and D. B. Drachman, *Science* **196**, 527 (1977); D. B. Drachman, C. W. Angus, R. N. Adams, J. Michelson, G. J. Hoffman, *N. Engl. J. Med.* **298**, 1116 (1978).
4. For rat myotubes, we define intact AChR clusters as intensely fluorescent patches measuring more than 10 μm^2. The mean measured value ± standard deviation of 484 myotubes containing AChR clusters was 253.4 ± 39.2 μm^2. The AChR microaggregates are defined as intensely fluorescent speckles measuring 2 to 9 μm^2. The mean ± standard deviation measured value of 462 myotubes containing AChR microaggregates was 4.0 ± 2.2 μm^2.
5. D. Yaffee, *Curr. Top. Dev. Biol.* **4**, 37 (1969).
6. P. Ravdin and D. Axelrod, *Anal. Biochem.* **80**, 585 (1977).
7. H. F. Deutsch, in *Methods in Immunology and Immunochemistry*, C. A. Williams and M. W. Chese, Eds. (Academic Press, New York, 1967), p. 319.
8. R. J. Bloch and B. Geiger, *Cell* **21**, 25 (1980).
9. E. Frank and G. D. Fischbach, *J. Cell Biol.* **83**, 143 (1979).
10. We used a modified form of the *t*-test for comparison of means drawn from populations of

unequal variances and sample sizes. Calculations were done by the method of F. E. Satterthwaite [*Biom. Bull.* **2**, 110 (1946)] as described in G. W. Snedecor and W. G. Cochran, *Statistical Methods* (Iowa State Univ. Press, Ames, ed. 7, 1980), pp. 96–98.
11. J. L. Goldstein, R. G. Anderson, M. D. Brown, *Nature (London)* **279**, 679 (1979); M. C. Willingham and I. Pastan, *Cell* **21**, 67 (1980).
12. V. A. Lennon, in *Cholinergic Mechanisms and Psychopharmacology*, D. J. Gender, Ed. (Plenum, New York, 1978), pp. 77–92; J. P. Merlie, S. Heinemann, J. M. Lindstrom, *J. Biol. Chem.* **254**, 6320 (1979); C. G. Reiness, C. B. Weinberg, Z. W. Hall, *Nature (London)* **274**, 68 (1978); D. Axelrod, *Proc. Natl. Acad. Sci. U.S.A.* **77**, 4823, (1980).
13. We thank Dr. S. A. Berman for carrying out the statistical computations and the reviewers for helpful comments. We are grateful to Mannie Steglich and Kim Seger for technical assistance. This project was supported by the Muscular Dystrophy Association and the Kleberg Foundation.
* To whom requests for reprints should be addressed.

4 January 1982; revised 28 September 1982

Sex Differences in Dendritic Structure in the Preoptic Area of the Juvenile Macaque Monkey Brain

Abstract. *Quantitative analysis of Golgi-stained neurons in the preoptic area of the brain of prepuberal* Macaca fascicularis *monkeys indicated structural differences between males and females. Neurons of males had more dendritic bifurcations and a higher frequency of spines. The bifurcation difference appeared in all cell types and was concentrated in the ventrolateral preoptic area. The spine difference was greatest in the central region of the preoptic area. No differences in gross measurements of this brain region were found. These results suggest that sexual dimorphism in the function of the monkey preoptic area may be based on differences in neuronal structure.*

Sex differences in adult mammalian reproductive physiology and behavior depend largely on differences in the organization of the brain, which are activated in the adult by circulating hormones (*1*). To a great extent, these sex differences in brain organization arise in response to gonadal steroid hormones present in the circulation during sensitive periods before or after birth (*2*). Recent research has indicated that sexual dimorphism in brain function may reflect differences in brain structure. For example, the preoptic area of the hypothalamus, which appears critical to male copulatory behavior and which is also involved in phasic female endocrine regulation in rodents (*3, 4*), exhibits sexual dimorphism in synaptic termination patterns (*5*), regional cell size and packing density (*6*), and dendritic density patterns (*7*). Sex differences have also been demonstrated in other parts of the rodent brain (*8*) and in the size of certain brain nuclei and one type of nerve cell in avian species (*9*).

We know relatively little about sex differences in the structure of the primate brain. There are sex differences in the overall size of the brain in humans and other primates (*10*), and there is evidence for human sex differences in morphological brain asymmetry (*11*). At a finer structural level, the only primate sex difference reported to date is in larger nerve cell nuclei in the amygdala of male than of female squirrel monkeys (*12*). These were intact adults whose gonads were releasing different hormones. Thus the nuclear size differences could reflect dynamic responses to circulating hormones rather than a stable sex difference (*13*). Because the preoptic area shows the greatest variety of reported structural dimorphisms in rodents, it seems a likely site for structural dimorphism at the cellular level in primates. This region is essential to normal male sexual behavior in macaques. Although it appears to be unnecessary for cyclic gonadotrophin regulation in primates in contrast to rodents (*3*), it probably plays a modulatory role (*14*). We used quantitative measurements of Golgi-stained neurons in the juvenile macaque monkey preoptic area and report here evidence for structural sexual dimorphism prior to the age of onset of adult sex differences in circulating hormones, which might affect these measures (*15*).

Four male and four female *Macaca fascicularis* monkeys, between 8 months and 2 years of age, were used. The preoptic area (POA) and surrounding tissue was dissected from the brain, block-stained according to a Golgi-Cox procedure (*16*), embedded in celloidin, and sectioned at a thickness of 100 μm in the coronal plane. Each subject was assigned a numerical code that did not reveal its sex. For sampling purposes, the POA was defined as a rectilinear solid lying under the anterior commissure (*17*). All well-impregnated neurons whose processes were not grossly attenuated by sectioning or otherwise obscured were traced by hand at ×500 magnification using a camera lucida microscope attachment. No attempt was made to follow dendritic processes in adjacent sections. Neurons were subclassified on the basis of dendritic spine frequency (*18*). (The location of each soma with regard to the brain's midline and the center of the anterior commissure was also recorded.) A total of 809 neurons from females and 980 neurons from males were drawn. The drawings were analyzed by counting and measuring the projected length of each dendritic branch. Branches were grouped in terms of their order away from the cell body, where first order refers to a branch from the cell body, second order, a branch beyond a bifurcation, and so forth.

The POA neurons were predominantly bipolar cells with a relatively simple dendritic field. Two major types of sex differences were evident. (i) There were approximately 20 percent more dendritic branches per neuron in males than in females (Table 1). The mean number of branches in every male exceeded that in every female. There was no statistical difference in the number of branches

Table 1. Brain measurements. Data are expressed as weighted mean ± standard error of the mean based on four individual subject means (*19*). Abbreviations: M, male; F, female; S, sparse; CC, corpus callosum; AC, anterior commissure; and IC, internal capsule.

Sex	Branches per neuron					Dendritic length (μm)	Percent neurons classified			Gross brain size	
	Order				Total		S	Intermediate	Spiny	CC to AC (mm)	Midline to IC (mm)
	1	2	3	4							
M	2.41 ± 0.04	3.05 ± 0.12	1.26 ± 0.10	0.26 ± 0.05	7.02 ± 0.29	299.4 ± 13.1	32.3	44.2	23.5	6.31 ± 0.06	2.36 ± 0.09
F	2.39 ± 0.02	2.64 ± 0.11*	1.01 ± 0.10	0.14 ± 0.04	6.19 ± 0.27†	277.2 ± 8.2	38.6	40.9	20.5‡	6.16 ± 0.08	2.44 ± 0.10

*$F(1, 6) = 6.58$; $P < .05$. †$F(1, 6) = 6.00$; $P < .05$. ‡χ^2 (2) = 7.4; $P < .025$ (*21*).